<u>**Supplementary Information**</u>

Genome-wide Meta-analysisUnravels Novel Interactionsbetween

Magnesium Homeostasis andMetabolic Phenotypes

<u>**Table of contents:**</u>

Supplementary Methods

Supplementary Figures 1-10

Supplementary Tables 1-8

Supplementary References

SUPPLEMENTARY METHODS

GWAS Cohorts

CoLaus is a population-based cohort with baseline examination conducted between 2003 and 2006. It includes 6,184 individuals of European descent aged 35-75 years randomly selected from the registry of the city of Lausanne [1]. The _CROATIA-Vis_ study, Croatia, is a family-based, cross-sectional study in the isolated island of Vis that included 1,056 examinees aged 18-93. Blood samples were collected in 2003 and 2004 [2]. The _CROATIA-Korcula_ study, Croatia, is a family-based, cross-sectional study in the isolated island of Korcula that included 965 examinees aged 18-95. Blood samples were collected in 2007 [3]. The _CROATIA-Split_ study, Croatia, is population-based, cross-sectional study in the Dalmatian city of Split that so far includes 1,012 examinees aged 18-95. Blood samples were collected in 2009 -2011 [4]. The _Lothian Birth Cohort 1936_ (LBC1936) consists of 1,091 relatively healthy older participants, most of whom took part in the Scottish Mental Survey of 1947 at the age of about 11 years. At a mean age of 69.5 years (SD 0.8) they were recruited to a study investigating influences on cognitive ageing [5]. A second wave of cognitive and physical testing occurred at approximately 73 years of age at which time a urine sample was collected [5, 6]. The _INGI-Val Borbera_ population is a collection of 1,785 genotyped samples (18-102 years) collected in the Val Borbera Valley, a geographically isolated valley located within the Appennine Mountains in Northwest Italy [7]. The _INGI-Carlantino_ study is a population-based, cross-sectional study in a village situated in the Southeastern part of the Apennines in a hilly area of the Puglia region. Main study characteristics are summarized in Suppl. Table 4, genotyping details on Suppl. Table 5.

Micro-dissection studies in mouse kidney

Well-characterized tubular segments were microdissected from mouse kidneys as described previously [8]. Kidneys from male C57BL/6J mice were dissected and minced before incubation with 0.1% (_w/v_) type 2 collagenase solution that contained 100 μg/ml soybean trypsin inhibitor for 30 min at 37°C. After digestion, the supernatant was sieved through 250- and 80-μm nylon filters. Nephron fragments remained in the 80-μm sieve and were resuspended by flushing. Distinct segments [glomeruli (GLOM), proximal convoluted and straight tubules (PCT and PST respectively), thick ascending loop of Henle (TAL), distal convoluted tubule (DCT) and collecting duct (CD)] were isolated upon their morphologic features. Three collections were snap-frozen in liquid nitrogen and conserved at -80°C.

Immunohistochemistry

Nephron immunohistochemistry was performed as described previously[9, 10]. In short, co-staining for ARL15, breast cancer resistance protein (BCRP), Tamm-Horsfall protein (TH), thiazide sensitive Na^+-Cl^- cotransporter (NCC) and aquaporin-2 (AQP2) was performed on 5-µm sections of fixed frozen mouse (C57BL/6J) kidney samples. The sections were incubated for 16 h at 4°C with the following primary antibodies: rabbit anti-ARL15 (1:100, Sigma Chemical Co., St Louis, USA), rat anti-BCRP (1:250 [10]), sheep anti-TH (1:750 [10]), rabbit anti-NCC (1:50 [11]) or rabbit anti-AQP2 (1:1000, kindly provided by Dr. Deen, Nijmegen, The Netherlands). For detection, kidney sections were incubated with Alexa Fluor-conjugated secondary antibodies. Images were taken with a Zeiss Axio Imager 1 microscope (Oberkochen, Germany) equipped with a HXP120 KublerCodix fluorescence lamp and a Zeiss AxiocamMRm digital camera.

Cell culture and transfection

Human embryonic kidney 293 (HEK293) cells were grown at 37°C in DMEM (Biowhittaker Europe, Vervier, Belgium) supplemented with 10% (*v/v*) FCS (PAA Laboratories, Linz, Austria), non-essential amino acids (AAs), and 2 mM L-glutamine in a humidified 5% (*v/v*) CO_2 atmosphere.

Cells were seeded in 12-well plates and subsequently transfected with a total of 1.25 µg of cDNA (per well in a 12 wells plate) using Lipofectamine 2000 (Invitrogen, Breda, The Netherlands). HA-tagged human TRPM6 was in the pCINeo-IRES-GFP mammalian expression vector [12]. A human ARL15 clone was obtained from Source BioScience (Berlin, Germany) and subcloned into the pCINeo-IRES-mCherry vector, used for transfections. The T46N mutation was inserted in the ARL15 construct using the QuikChange site-directed mutagenesis kit (Stratagene, La Jolla, CA, USA) according to the manufacturer's protocol. All constructs were verified by sequence analysis. Mock conditions were obtained by transfecting the empty pCINeo-IRES-mCherry vector. Approximately 36 h after transfection, cells were seeded on glass coverslips coated with 50 µg/ml fibronectin (Roche Diagnostics, Mannheim, Germany). Experiments were started 2 h after seeding the cells. Cells displaying both GFP and mCherry fluorescence were chosen for recording.

Electrophysiology

All experiments were performed at room temperature. Whole-cell recordings were undertaken and analyzed using an EPC-9 amplifier and the Patchmaster software (HEKA electronics,

Lambrecht, Germany). The sampling interval was set to 100 μs (10 kHz) with a low-pass filter set at 2.9 kHz. Pipettes were pulled from thin wall borosilicate glass (Harvard Apparatus, March-Hugstetten, Germany) and had resistance between 1 and 3 MΩ when filled with the pipette solution. Series resistance compensation was set to 75-95% in all experiments. Currents were elicited by a series of 500 ms voltage ramps (from -100 to +100 mV) applied every two seconds from a holding voltage of 0 mV. Current densities were obtained by normalizing the current amplitude to the cell capacitance.

The extracellular solution contained (in mM): 150 NaCl, 1 $CaCl_2$, 10 HEPES and pH adjusted to 7.4 using NaOH. The pipette solution was made of (in mM): 150 NaCl, 10 Na_2EDTA, 10 HEPES and pH adjusted to 7.2 using NaOH.

Conservation of ARL15 proteins

TBLASTN searches were performed on the mouse, cow and zebrafish genome database at NCBI (http://blast.ncbi.nlm.nih.gov/Blast.cgi) using the human ARL15 as query AA sequence. Sequences with a significant homology with human ARL15 were selected. Multiple sequence alignments were carried out using ClustalW (http://www.ebi.ac.uk/Tools/clustalw/) and the degree of AA conservation across species was discerned.

Distribution of *Arl15* gene expression and dietary Mg^{2+} challenge in mice

To study the tissue distribution of *Arl15* gene expression, three C57BL/6J mice were sacrificed; lung, bone, kidney, peritoneum, stomach, brain, heart, liver and muscle tissues were collected. The dietary Mg^{2+} challenge was performed on age- and gender-matched C57BL/6J wild type (WT) littermates. Mice were housed in a temperature- and light-controlled room with *ad libitum* access to standard pellet chow (SSNIFF Spezialdiäten, Soest, Germany) and deionized drinking water for 4 weeks until the start of the experiment. Three groups of mice were next fed a control diet (0.19% (*w/w*) Mg; n = 10), a Mg^{2+}-deficient diet (0.0005% (*w/w*) Mg; n = 10), or a Mg^{2+}-enriched diet (0.48% (*w/w*) Mg; n = 10) (SSNIFF Spezialdiäten, Soest, Germany) for 10 days. Mice were housed individually in metabolic cages overnight at baseline, day 5 and day 10 for urine collection (16 h sampling). Venous blood samples were obtained from the inferior vena cava during sacrifice at day 10, and kidneys and intestine (ileum and caecum) were harvested as previously described [13]. All protocols were conducted in accordance with the National Research Council Guide for the Care and Use of Laboratory animals and were approved by the local Ethics Committee.

Distribution of *arl15b* gene expression and dietary Mg^{2+} challenge in zebrafish

Zebrafish from the Tupfel long-fin (TLF) strain were used for experimentation. For the study of the tissue distribution of the highly conserved ARL15 zebrafish ortholog (*arl15b*) in adult zebrafish tissues, 3 females and 3 males were dissected following anaesthesia (0.1% (*v/v*) 2-phenoxyethanol (Sigma Chemical Co., St Louis, USA)) and brain, ovary, gills, testis, heart, spleen, kidney, gut, operculum, scales and liver tissues were collected and stored at -80°C until analysis. In 5 days post-fertilization (dpf) larvae, animals were anaesthetised with tricaine/Tris pH 7.0 solution and pronephric tissue was isolated with fine-point needles under the microscope (Leica Microsystems Ltd). After removal of the yolk and swim bladder, the pronephros could be distinguished by the pigments that surround the pronephric tubules (Suppl. Fig. 8). Then, pronephric-enriched tissue was scratched and subsequently aspirated with a Pasteur pipette. Samples were constituted by 10 pronephros each, which were stored at -80°C until further analysis. Control genes were used to verify the purity of the pronephric tissue isolated:*ncc*, uniquely expressed in the pronephros[14], served as positive control; and *ncc-like*, whose gene expression is restricted to the skin [15], served as negative control.

To study the regulation of *arl15b* gene expression by the Mg^{2+} status in zebrafish ionoregulatory tissues (gills, kidney and gut), fish Mg^{2+} balance was challenged by different Mg^{2+} diets as previously reported [16]. Briefly, 27 adult zebrafish were weighed and randomly divided into 3 groups of 9 animals each and kept in 3 separate 2-liter tanks. During 2 weeks (acclimation to control conditions), all fish were fed aMg^{2+}-control diet (Hope Farms, Woerden, The Netherlands; 0.07% (*w/w*) Mg) at a daily ration of 2% (*w/w*) of the total body weight. After this period, for 2 groups, the control diet was replaced by aMg^{2+}-deficient diet (Hope Farms; 0.01% (*w/w*) Mg) or a Mg^{2+}-enriched diet (Hope Farms; 0.7% (*w/w*) Mg). These 2 groups were kept under these feeding regimes for 3 weeks, while the remaining group (fed aMg^{2+}-control diet) served as a control. At the end of this period, all groups were sampled. Sampling took place 24 h after the last feeding. Fish were anaesthetised in 0.1% (*v/v*) 2-phenoxyethanol (Sigma). After anaesthesia, death of animals was induced by spinal transaction and organs were collected, immediately frozen in liquid nitrogen and stored at -80°C until analysis. All animal procedures detailed here were performed in accordance with national and international legislation and were approved by the ethical review committee of the Radboud University Nijmegen.

Knockdown of the zebrafish ortholog of human ARL15 and rescue experiments

WT TLF zebrafish were bred and raised under standard conditions (28.5°C and 14 h of light: 10 h of dark cycle) in accordance with international and institutional guidelines. Zebrafish eggs were obtained from natural spawning. The following splice-site blocking morpholinos (MOs) were designed to knockdown *arl15b* expression: 5'-AAACACTGAAAGACGGGACAAAGAC-3' and GTTAAGCGAGTATTAGGTTACCTCT-3' (Gene Tools, Philomath, OR, USA), designated as exon 3 and 4 skipping *arl15b*-MO respectively. A standard mismatch MO, directed against a human β-globin intron mutation, 5'-CCTCTTACCTCAGTTACAATTTATA-3', was also used in the experiments to control for toxic effects of the MO molecule. MOs were diluted in deionized, sterile water supplemented with 0.5% (*w/v*) phenol red and injected in a volume of 1 nl into the yolk of one- to two-cell stage embryos using a Pneumatic PicoPump pv280 (World Precision Instruments, Sarasota, FL, USA). WT embryos (uninjected) were also included in the experiments to control for the effects of the injection procedure *per se*. To determine the most effective dose of the *arl15b*-MO, 0.5, 1 and 2 ng *arl15b*-MO; and 2, 4 and 8 ng *arl15b*-MO were injected in two sets of experiments. In these experiments, control embryos were injected with 2 or 8 ng of the standard mismatch control-MO (the highest dose for each set of experiments respectively). After injection, embryos from the same experimental condition were placed in 3 Petri dishes and cultured at 28.5°C in E3 embryo medium (5 mMNaCl, 0.17 mMKCl, 0.33 mM $CaCl_2$, 0.33 mM $MgSO_4$), which was refreshed daily.

Morphological phenotypes characterizing kidney function and yolk metabolization were analyzed in larvae at 5 dpf. Larvae were classified into different classes of phenotypes on the basis of comparisons with stage-matched control embryos (injected with the control-MO) of the same clutch. In *arl15b*morphant larvae (5 dpf), 4 different phenotypes were distinguished: normal; mild, larvae with mild-moderate pericardial edema (indicative of kidney dysfunction) and metabolic defects (poor metabolization of the yolk); moderate, moderate pericardial edema accompanied by kidney cysts in approximately 75% of the cases, metabolic defects (poor metabolization of the yolk) and cardiovascular defects (poor blood circulation in the tail); severe, severe pericardial edema accompanied by kidney cysts in approximately 80% of the cases, metabolic defects (poor metabolization of the yolk) and cardiovascular defects (poor blood circulation or absence in the tail and severe bradychardia (heart beat rate below 100 beats per minute)). Representative images were obtained with a DFC450C camera (Leica Microsystems Ltd) after anaesthetising larvae with tricaine/Tris pH 7.0 solution.

For electrolyte measurements or RNA isolation, 7-10 zebrafish larvae were pooled as one sample. Samples were then snap frozen in liquid nitrogen and stored at -80°C in order to ensure euthanasia of animals.

In vivo cRNA rescue experiments were performed with human WT ARL15 and dominant negative mutant (T46N) ARL15 cRNAs. Constructs were sub-cloned into the pT7Ts expression vector, suitable for rescue experiments in zebrafish [17], and cRNAs were prepared using the mMESSAGEmMACHINE Kit (Ambion, Austin, TX, USA) according to the manufacturer's instructions. The cRNAs, in an amount of 50 pg, as based on previous studies [18, 19], were (co)injected together with MOs as described above. Zebrafish larvae were phenotyped at 5 dpf.

Electrolyte measurements in animal studies

In mice, urinary creatinine and electrolytes as well as plasma urea and creatinine (enzymatic determination) were measured on a SynchronUnicelDxC 800 analyzer (Beckman Coulter, Brea, USA).In zebrafish, sample processing started by washing twice the samples with nanopure water in order to avoid contamination of remaining waterborne Mg^{2+}. Fish were then dried and digested as described previously [19]. The total Mg content in each sample was determined with a colorimetric assay (Roche). Within-run precision and accuracy was controlled by means of an internal control Precinorm (CV = 0.8%). Furthermore, samples were normalized by protein content, which was determined with the Pierce BCA protein assay kit (Pierce Biotechnology, Rockford, IL, USA).

RNA isolation and cDNA synthesis

In mouse, total RNA was extracted from different tissues using the Aurum[TM]Total RNA Fatty and Fibrous TissueKit (Bio-Rad, Hercules, CA), following the manufacturer's protocol. In zebrafish, RNA was isolated from zebrafish tissues and larvae using TRIzol reagent (Invitrogen, Carlsbad, CA, USA) according to the manufacturer's instructions in which glycogen (Fermentas GmbH, St. Leon-Rot, Germany) was used in order to maximize the RNA recovery. This method allowed the isolation of more than 3 µg RNA per tissue or whole-larvae sample (n = 7-10 larvae/sample), and of more than 200 ng RNA per pronephric samples (10 pronephros/sample). In both, mouse and zebrafish RNA samples, one µg of RNA, or 200 ng in the case of pronephric samples, was subjected to DNase treatment to prevent genomic DNA contamination and subsequently used to perform the reverse transcriptase reaction.

Reverse transcription quantitative polymerasechainreaction (RT-qPCR)

Changes in target genes mRNA levels were determined by relative RT-qPCR following the MIQUE guidelines [20] with a CFX96[TM] Real-Time PCR Detection System (Bio-Rad Laboratories, Hercules, CA) using iQ[TM]SYBR Green Supermix (Bio-Rad) detection of single PCR product accumulation. To study the effect of dietary Mg^{2+} on gene expression in mouse kidney, ileum and caecum, the geNorm algorithm was used with 5 reference genes to calculate the normalization factor (software geNorm version 3.4). The reference genes used encoded for β-actin (*Actb*), glyceraldehyde 3-phosphate dehydrogenase (*Gapdh*), peptidylprolyl isomerase A(*Ppia*), attachment region binding protein(*Arbp*) and hypoxanthine phosphoribosyltransferase 1 (*Hprt1*). In the rest of procedures with mice (tissue distribution and gene expression profile in different mouse nephron segments) and in the zebrafish studies, gene expression levels were normalized to the expression levels of the standard species-specific reference genes *Gapdh* (for mice [21, 22]) and elongation factor-1α (*elf1α*, for zebrafish [16, 23]). Here, relative mRNA expression was analysed using the Livak method ($2^{-\Delta\Delta Ct}$). Primer sequences are shown in Suppl. Table 8.

Efficacy of the splice-site blocking*arl15b*-morpholinos.To determine the efficacy of the splice blocking induced by the exon 3 skipping *arl15b*-MO, cDNA from 5 dpfcontrol (injected with 0.5 ng control-MO) and morphant (injected with 0.5 ng *arl15b*-MO) larvae was used for PCR analysis. The primers used were 5'-CGAGGTCACAGGGGTGTTTC-3' as forward primer and 5'-GACGAAGCGCTGTCCAAAAC-3' as reverse primer. Fragments thus obtained were extracted from a 1.5% agarose gel and Sanger-sequenced (Suppl. Fig. 9) to confirm the splice blocking induced.

In the case of the exon 4 skipping *arl15b*-MO, cDNA was generated from fish injected with 2 ng control or *arl15b*-MO. Primers used were 5'-CTGACGGGTTCTGGGAAGAC-3' as forward primer and 5'-ACCGTGCTTCCCTCTAGGAT-3' as reverse primer. Given the absence of a spliced-*arl15b* transcript in 2-5 dpf fish (as a result of nonsense-mediated decay of *arl15b* mRNA by the exon 4 skipping *arl15b*-MO,Suppl. Fig. 10), the efficacy of the approach was further studied by RT-qPCR using specific primers that discriminate for the functional (non-spliced) *arl15b* transcript: the forward primer targets the exon 3-4 junction and the reverse primer targets exon 4 (Suppl. Table 8).

SUPPLEMENTARY FIGURES

Supplementary Figure 1.Manhattan plot from the GWAS on uMg-to-creatinine ratio for the CoLaus cohort.
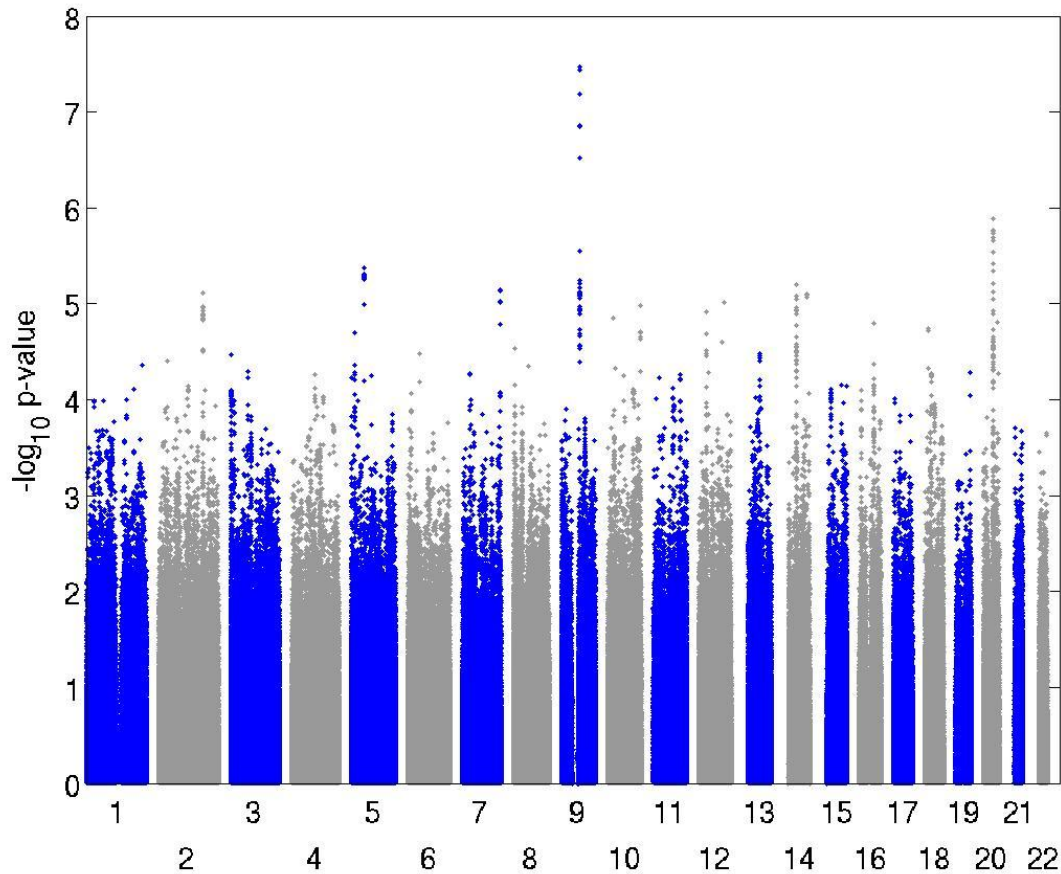

Manhattan plot showing -log10(P values) for all SNPs in the genome-wide association for normalized uMg-to-creatinine ratio in CoLaus (n=5,150), ordered by chromosomal position. The values correspond to the association of normalized uMg-to-creatinine ratio, including as covariates age, sex and the first principal components generated from all genotypes to take population structure into account. One locus (*TRPM6*) reached genome-wide significance ($P< 5\times10^{-8}$).

**Supplementary Figure 2.QQ plot and conditional analyses for the uMg-to-creatinine ratio.**

(**a**)QQ plot from the meta-analysis of uMg-to-creatinine ratio.
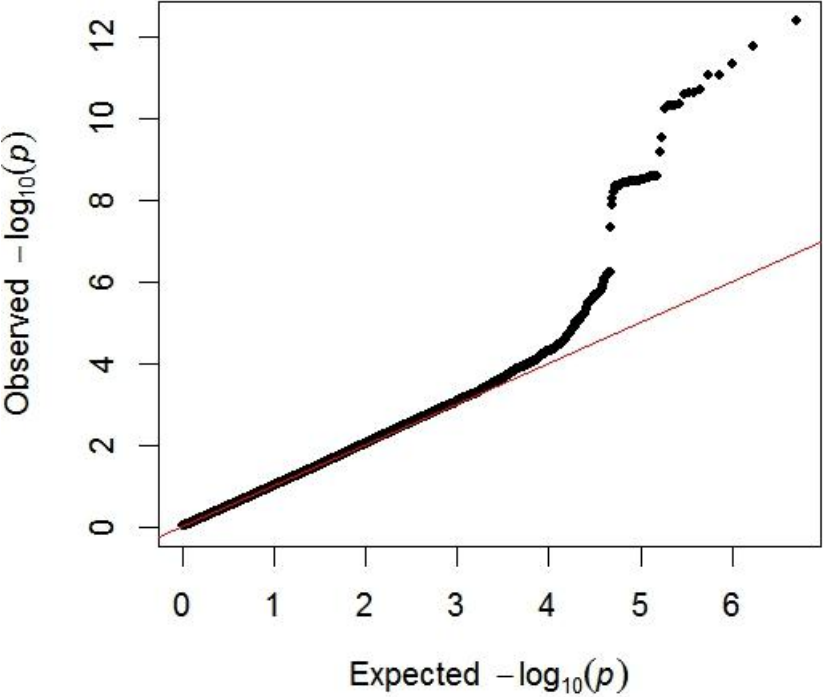
(**b**) Zoom plot showing the *TRPM6* region's associations to uMg-to-creatinine ratio after conditioning the analysis for rs3824347.
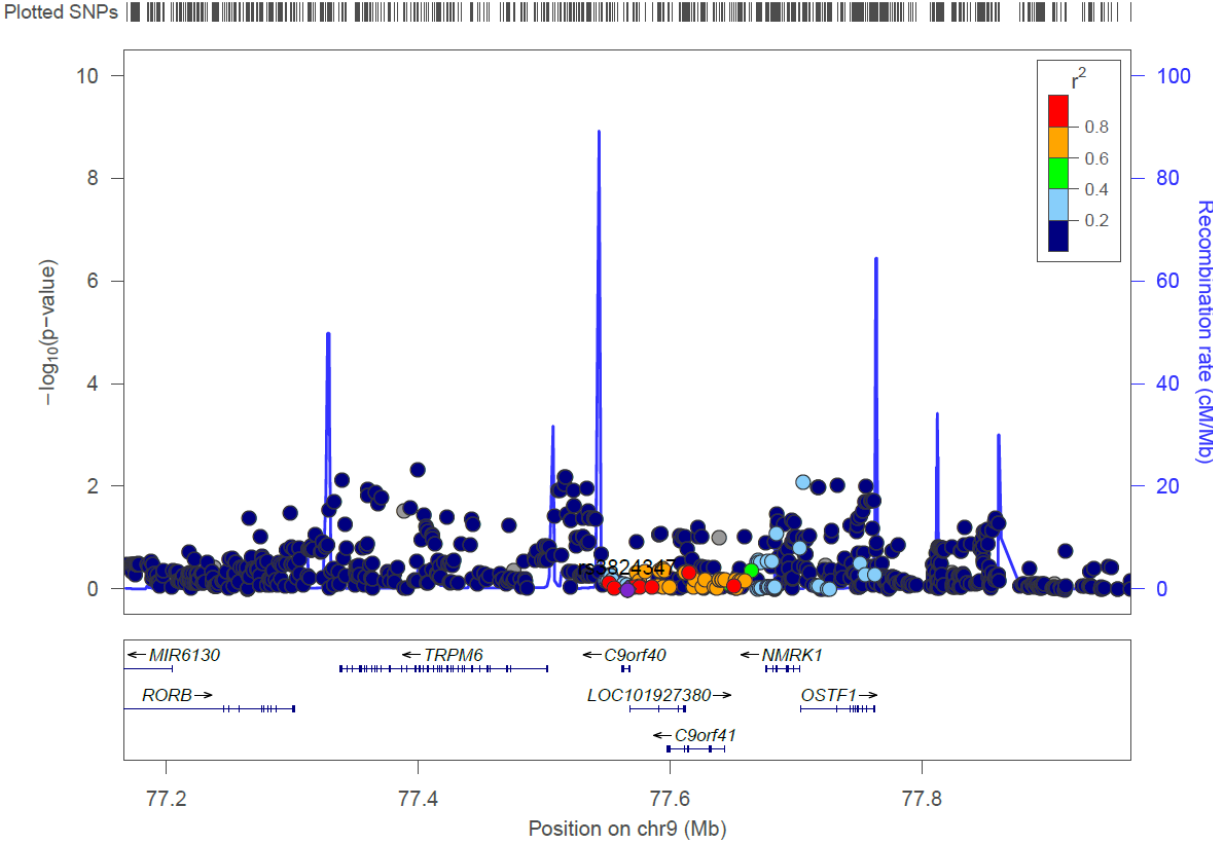
(**c**) Zoom plot showing the *ARL15* region's associations touMg-to-creatinine ratio after conditioning the analysis for rs35929.
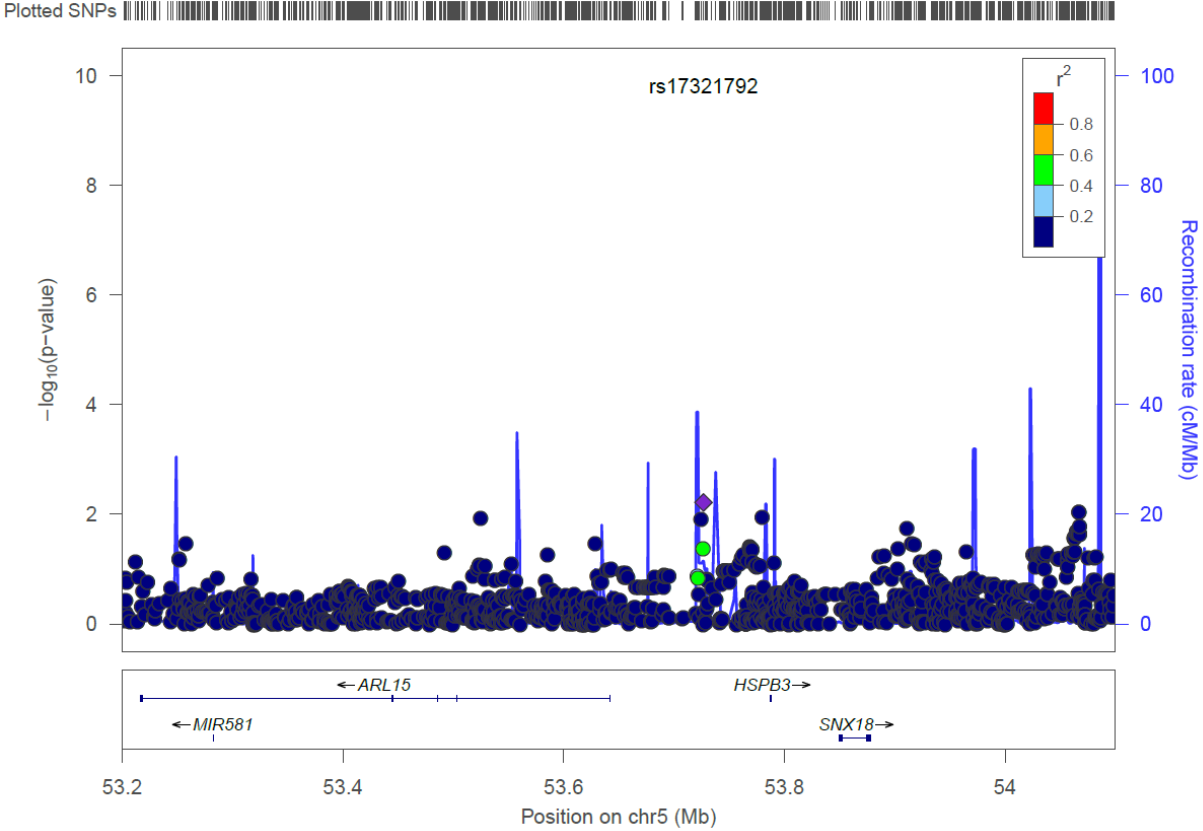
Supplementary Figure 3.Manhattan plot from the GWAS on serum Mg^{2+} levels for the meta-analysis.

a

b
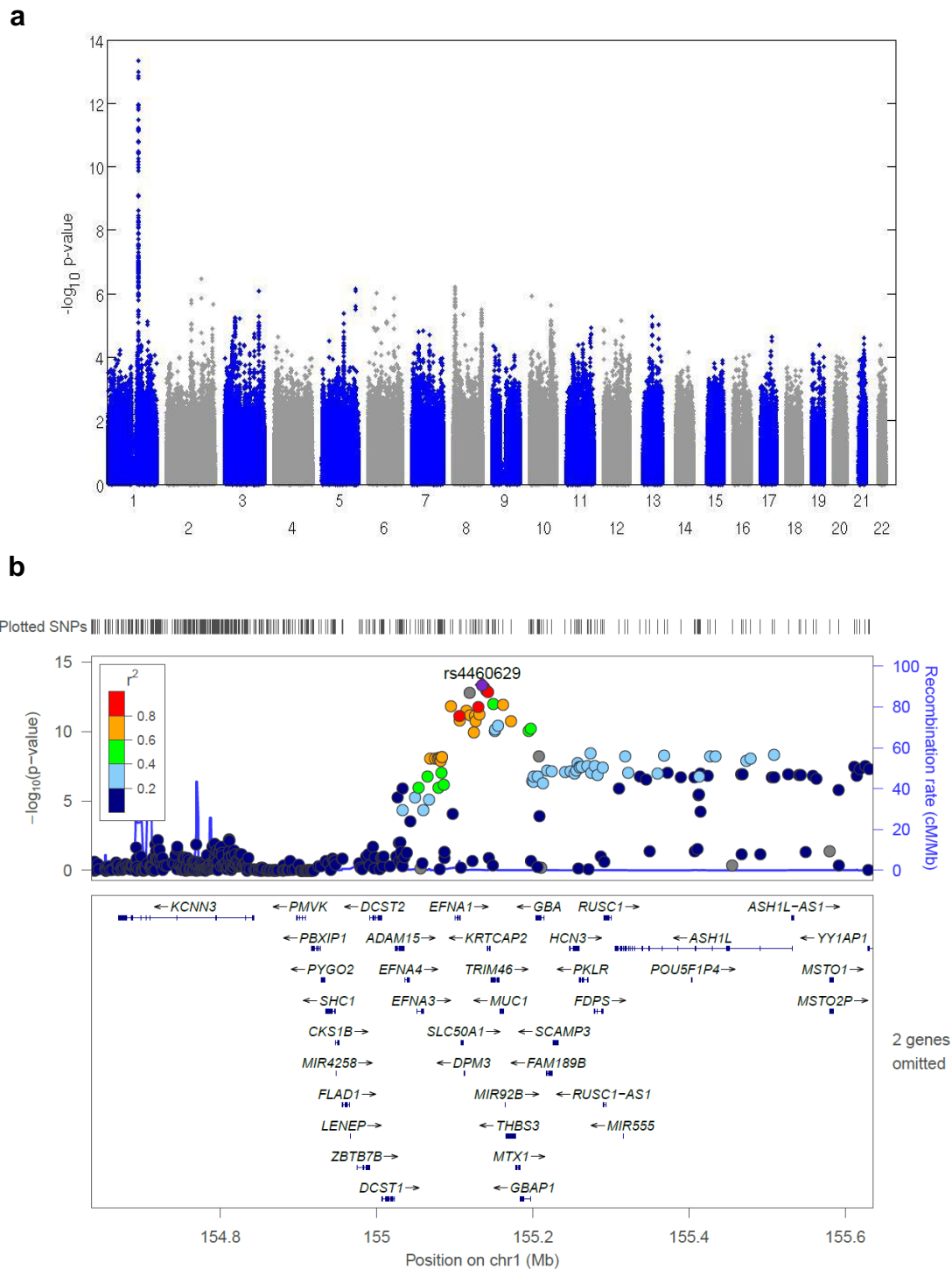
(**a**) Manhattan plot showing all –log10(*P* values) for the combined analysis of the GWAS on serum Mg^{2+}, ordered by chromosome position. A locus on chromosome one reaches genome-wide significance. (**b**) Regional association plot of the region on chromosome one identified on the Manhattan plot on panel A. It shows a gene-rich locus, with no obvious candidate for being the gene involved.

Supplementary Figure 4.Manhattan plot from the meta-analysis of fractional excretion of Mg^{2+} (FEMg) GWASs.
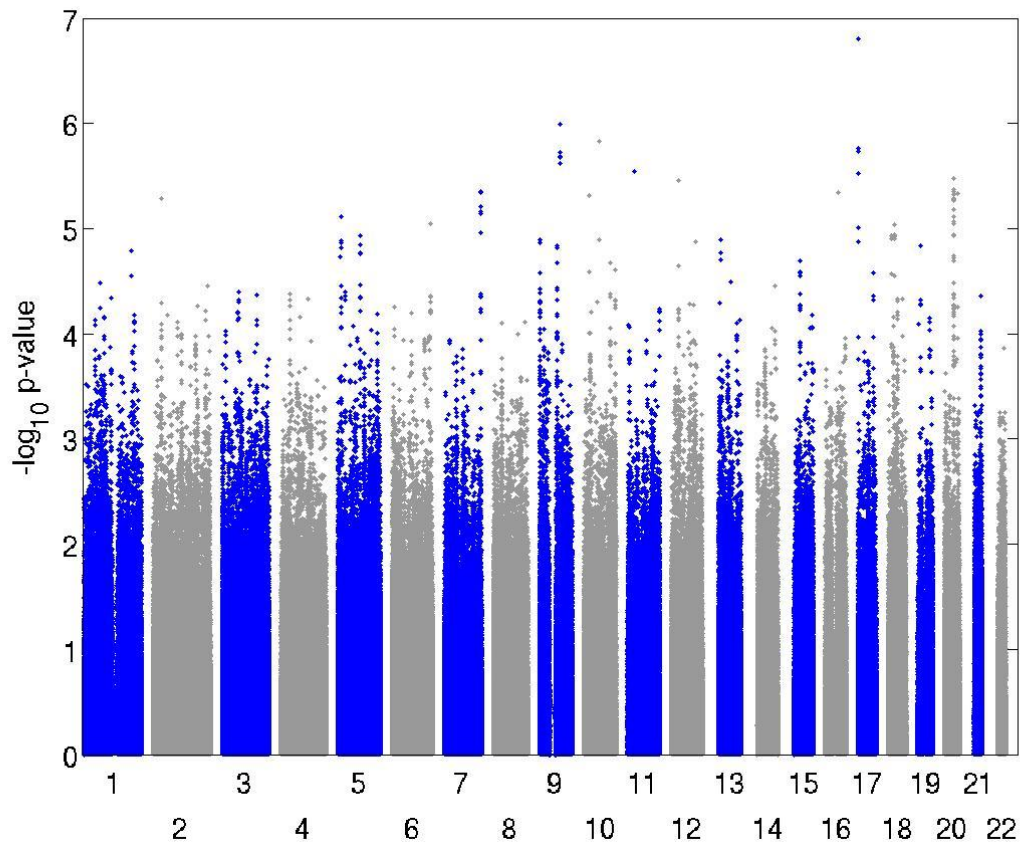
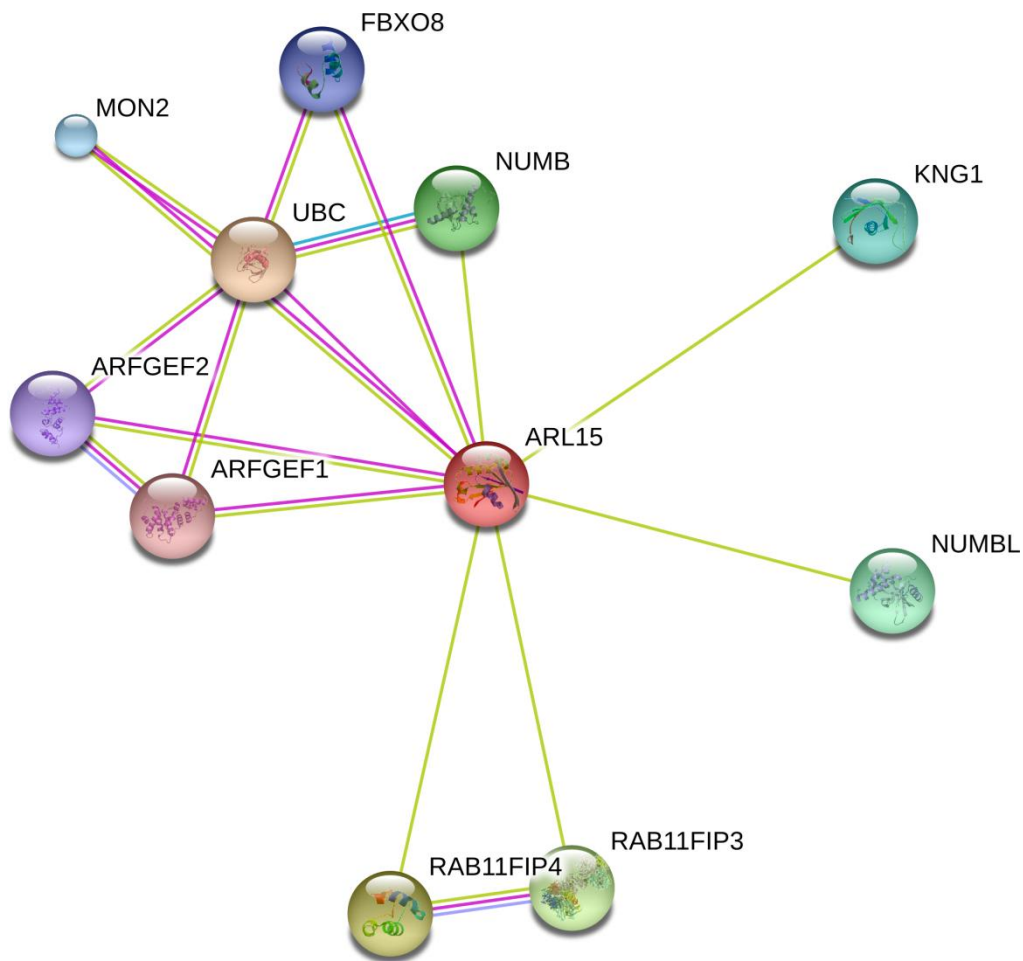Manhattan plot showing all −log10(P values) for the combined analysis of the GWAS on FEMg, ordered by chromosome position. No signal reaches genome-wide significance.

Supplementary Figure 5.Functional protein association network analyses for ARL15.

ARL15 interacts with regulators of endocytic (RAB11FIP4, UBC) and vesicular (ARFGEF1) trafficking, factors involved in maintenance of cell polarity (ARFGEF1), factors influencing sodium handling (KNG1) and regulators of ubiquitination (UBC). (http://string-db.org/cgi/network.pl?taskId=NPTdrqbgkFZS). Network nodes represent proteins, whereas different colored nodes refer to different proteins. Small nodes (MON2) refer to proteins of unknown 3D structure while large nodes represent proteins whose 3D structure is known or predicted (ARL15, KNG1, NUMBL, RAB11FIP3, RAB11FIP4, ARFGEF1, ARFGEF2, UBC, NUMB, FBXO8). Edges represent protein-protein associations: blue, interactions from curated databases (e.g. UBC-NUMB); magenta, experimentally determined interactions (e.g. ARL15-ARFGEF1, ARL15-ARFGEF2, ARL15-UBC, ARL15-MON2, ARL15-FBXO8); green, interactions derived from textmining (e.g. ARL15-RAB11FIP3, ARL15-RAB11FIP4, ARL15-NUMBL, ARL15-KNG1, ARL15-NUMB); purple, interactions deduced by protein homology (e.g. ARFGEF1-ARFGEF2).

Supplementary Figure 6.Tissue distribution of *Arl15* gene expression in mouse tissues and regulation of gene expression by dietary Mg^{2+} in mouse tissues relevant for Mg^{2+} handling.
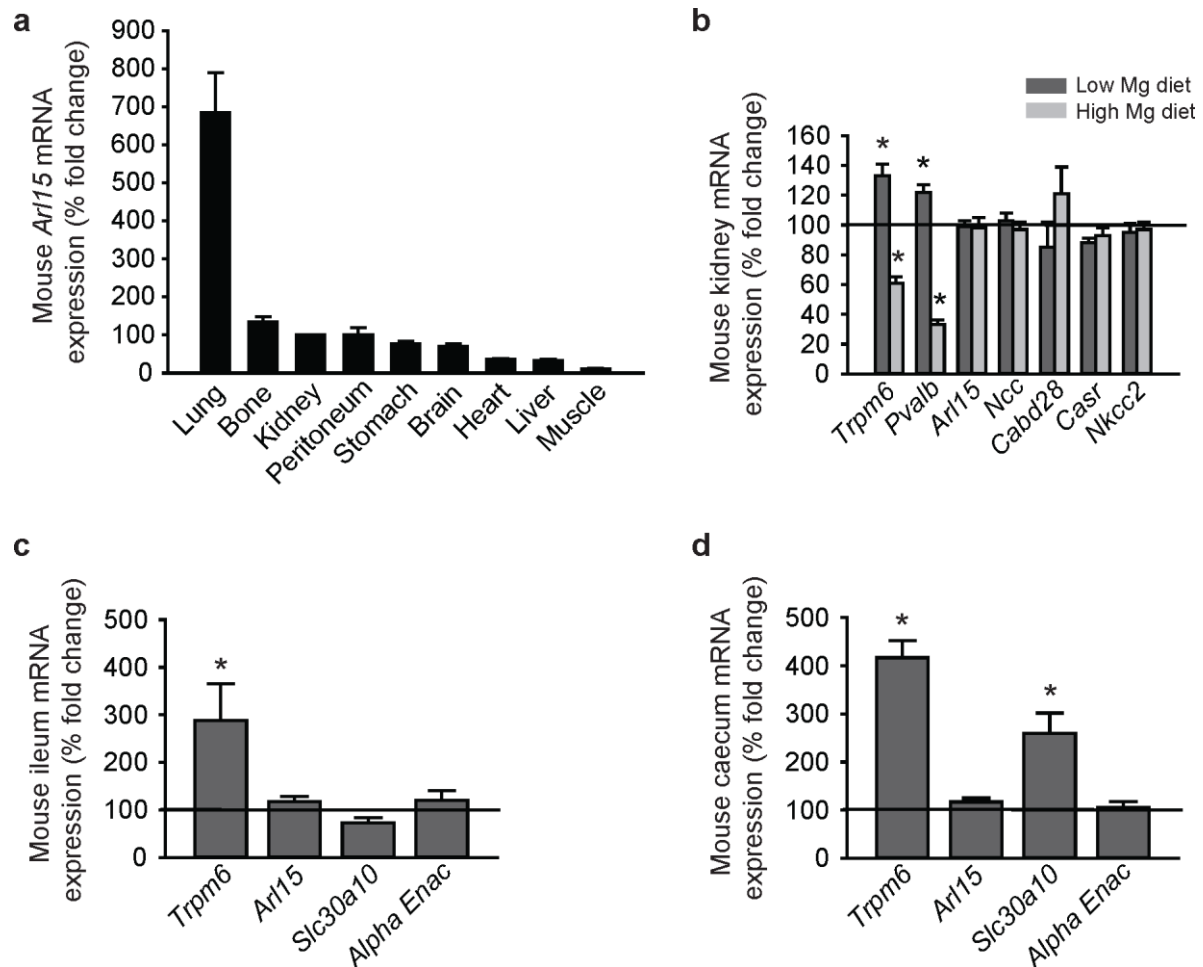
(**a**) Tissue distribution of *Arl15* gene expression in mouse tissues. Relative gene expression in mouse tissues and organs was analysed using the Livak method ($2^{-\Delta\Delta Ct}$), where results are normalized against the reference genes *Gapdh* and expressed relative (%) to the gene expression in the kidney, chosen as calibrator. Data are presented as mean ± SEM (n = 3). (**b-d**) Gene expression levels of*Trpm6*, parvalbumin (*Pvalb*), *Arl15*, the Na^{+}-Cl^{-} cotransporter (*Ncc*), calbindin D-28k (*Cabd28*), the calcium-sensing receptor (*Casr*) and the Na^{+}-K^{+}-Cl^{-} cotransporter isoform 2 (*Nkcc2*) in mouse kidney (**b**); of *Trpm6*, *Arl15*, the zinc transporter 10 (*Slc30a10*) and the alpha subunit of the epithelial sodium channel (*Alpha Enac*) in mouse ileum (**c**); and *Trpm6*, *Arl15*, *Slc30a10* and *Alpha Enac* in mouse caecum (**d**). Mice were fed a control diet (0.19% (*w/w*) Mg), a Mg^{2+}-deficient diet (0.0005% (*w/w*) Mg), or a Mg^{2+}-enriched diet (0.48% (*w/w*) Mg) for 10 days. Gene expression data were calculated using the geNorm algorithm and represent the mean fold difference (mean ± SEM, n = 10 for kidney and n = 5 for ileum and caecum) from the control group (mice on the control diet). $^{*}P < 0.05$ compared with the control group.

Supplementary Figure 7. The zebrafish Arl15b protein is a highly conserved ortholog of human ARL15 being its gene expression is magnesiotropic in kidney, gills and gut.

a

```
Human ARL15        1  --MSDLRITEAFLYMDYLCFRALCCKGPPPARPEYDLVCIGLTGSGKTSLLSKLCSESPD
Mouse ARL15        1  --MSDLRITEAFLYMDYLCFRALCCKGPPPARPEYDLVCIGLTGSGKTSLLSELCSESPE
Cow ARL15          1  --MSDLRISEAFLYMDYLCFRALCCKGPPPARPEYDLVCIGLTGSGKTSLLSKLCSESPD
Zebrafish Arl15b   1  --------------MLDYCFRTLCCKGPPPPRPEYDVVCIGLTGSGKTSLLSRLCSEATD
Zebrafish Arl15a   1  MSEHIQLSVALCRIGFYTCLQKLCCKAPPPPRPEYDVVCIGLSGAGKTSLLSRLCNEISD

Human ARL15       59  NVVSTTGFSIKAVPFQNAILNVKELGGADNIRKYWSRYYQGSQGVIFVLDSASSEDDLEA
Mouse ARL15       59  NVVSTTGFSIKAVPFQNAVLNVKELGGADNIRKYWSRYYQGSQGVIFVLDSASSEDDLET
Cow ARL15         59  SVVSTTGFSIKAVPFQNAILNVKELGGADNIRKYWSRYYQGSQGVIFVLDSASSEDDLET
Zebrafish Arl15b  47  NIVPTTGFSIKAVPFQNAILNVKELGGADSIKKYWSRYYQGSQGVVFVLDSASSEEDLEV
Zebrafish Arl15a  61  GTVPTTGFSIKAVPFENAILNVKELGGAETIKKYWSRYYQGSQGVVFVLNSAASDEEMEA

Human ARL15      119  ARNELHSALQHPQLCTLPFLILANHQDKPAARSVQEIKKYFELEPLARGKRWILQPCSLD
Mouse ARL15      119  ARNELHSALQHPQLCTLPFLILANHQDKPAARSVQEIKKYFELEPLARGKRWILQPCSLD
Cow ARL15        119  ARNELHSALQHPQLCTLPFLILANHQDKPAARSVQEVKKYFELEPLARGKRWILQPCSLD
Zebrafish Arl15b 107  ARTELHSALQHPQLCTLPFLILANHQDKPAARSVQEIKKYFELEPLARGKSWILEGSTVD
Zebrafish Arl15a 121  SRSELHLALQHPQLCTLPFLVLANHQDSPAARSVSEIRKFFELEPLARGKRWILAGTSTN

Human ARL15      179  DMDALKDSFSQLINLLEEKDHEAVRM
Mouse ARL15      179  DVDTLKDSFSQLINLLEEKDHEAVRM
Cow ARL15        179  DMEALKDSFSQLINLLEDHEAVRM--
Zebrafish Arl15b 167  NMTAVKESFAQLIHLLEEKDQETGRI
Zebrafish Arl15a 181  NMEDVKESFSQLISLLEEKEVLPSRI
```

b
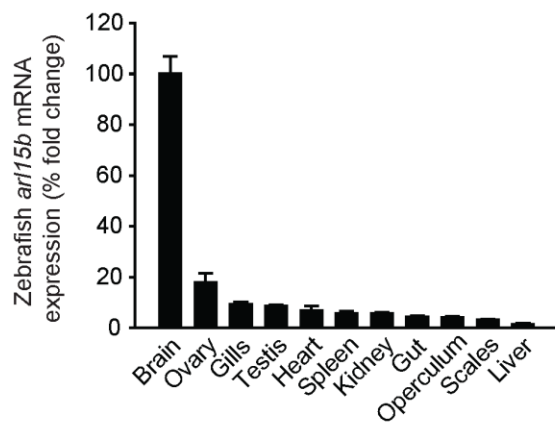
c

d

e

(**a**) Alignment of the human, mouse and cow ARL15 proteins (GenBank accession no. NP_061960, NP_766183 and NP_001014943 respectively) and zebrafish Arl15 paralogs: Arl15a and Arl15b (GenBank accession no. NP_001093503 and XP_001923547 respectively). Identical AAare boxed in black, conservative substitutions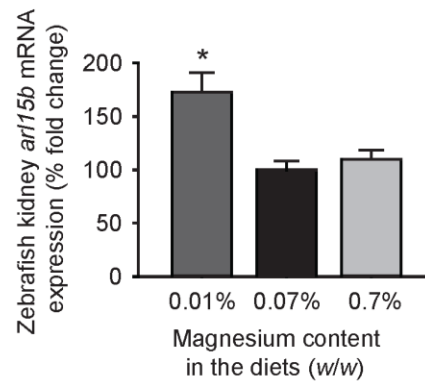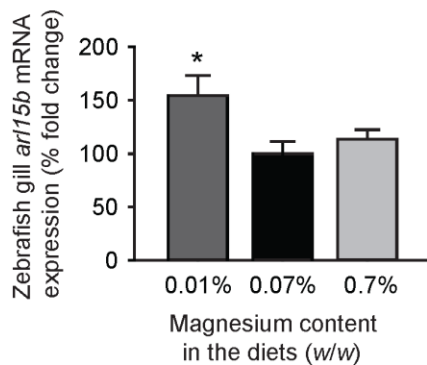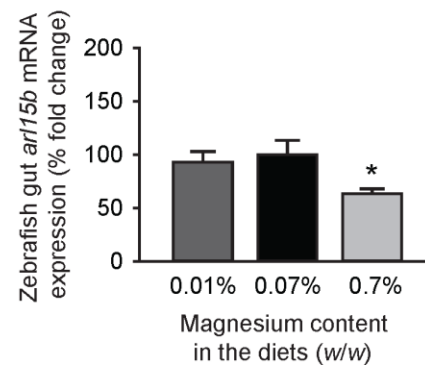 in gray. Sequence identity of zebrafish Arl15a with human, mouse and cow ARL15 is 68, 66 and 67% respectively. Zebrafish Arl15b displayed a strikingly high degree of AA conservation with its mammalian counterparts: 83, 81 and 79% with human, mouse and cow ARL15 respectively. (**b**) Tissue distribution of *arl15b* gene expression in zebrafish tissues. Relative gene expression in mouse and zebrafish tissues and organs was analysed using the Livak method ($2^{-\Delta\Delta Ct}$), where results are normalized against the translational *elf1α* and expressed relative (%) to the gene expression in the brain, chosen as calibrator. Data are presented as mean ± SEM (n = 6, except for the ovary and testis where n = 3). (**c-e**) Gene expression levels of *arl15b* in kidney (**c**), gills (**d**) and gut (**e**) ofzebrafish on a Mg^{2+}-deficient diet (0.01% (*w/w*) Mg), Mg^{2+}-control diet (0.07% (*w/w*) Mg)and Mg^{2+}-enriched diet (0.7%(*w/w*) Mg) for 21 days. Data werecalculated using the Livakmethod ($2^{-\Delta\Delta Ct}$) and theyrepresent the mean folddifference (mean ± SEM,n= 8-9) from the control group (fish on the control diet). $^{*}P <$ 0.05 was considered statistically significant when compared with the control group.

Supplementary Figure 8. The *arl15b* gene is expressed in the pronephric kidney of zebrafish larvae.
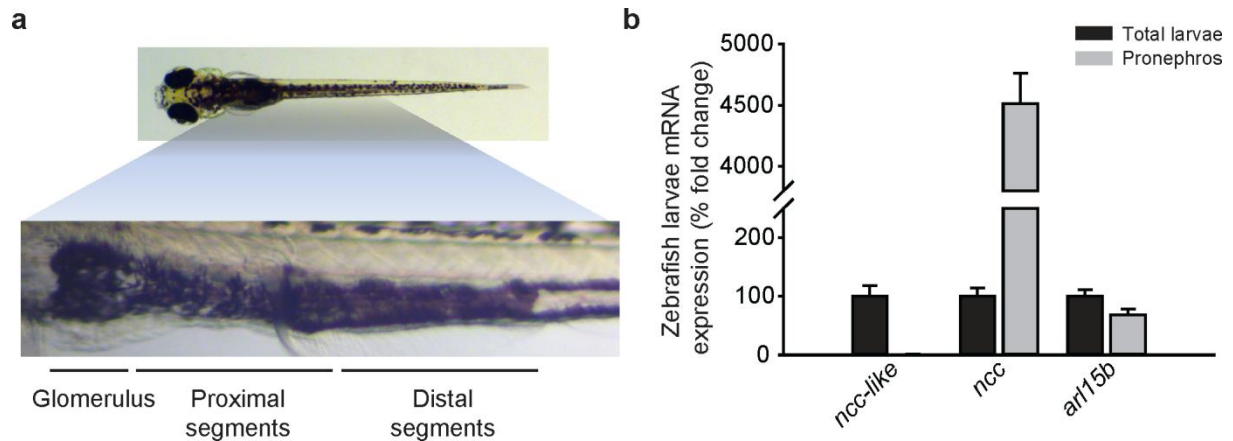
(**a**) The pronephros of 5 dpf zebrafish larva after dissection for collection of pronephric-enriched tissue. Pronephric tubules can be distinguished by the black pigments that develop around the tubuli. (**b**) Gene expression of *arl15b* and the control genes *ncc* (uniquely expressed in the pronephros, as positive control) and *ncc-like* (distinctly expressed in the skin, as negative control) in the pronephros and total larvae. Relative gene expression was analysed using the Livak method ($2^{-\Delta\Delta Ct}$), where results are normalized against the reference gene*elf1α* and expressed relative (%) to the gene expression in total larvae. Data are presented as mean ± SEM (n = 3).

Supplementary Figure 9.Efficacy of the exon 3 skipping *arl15b*-MO used.
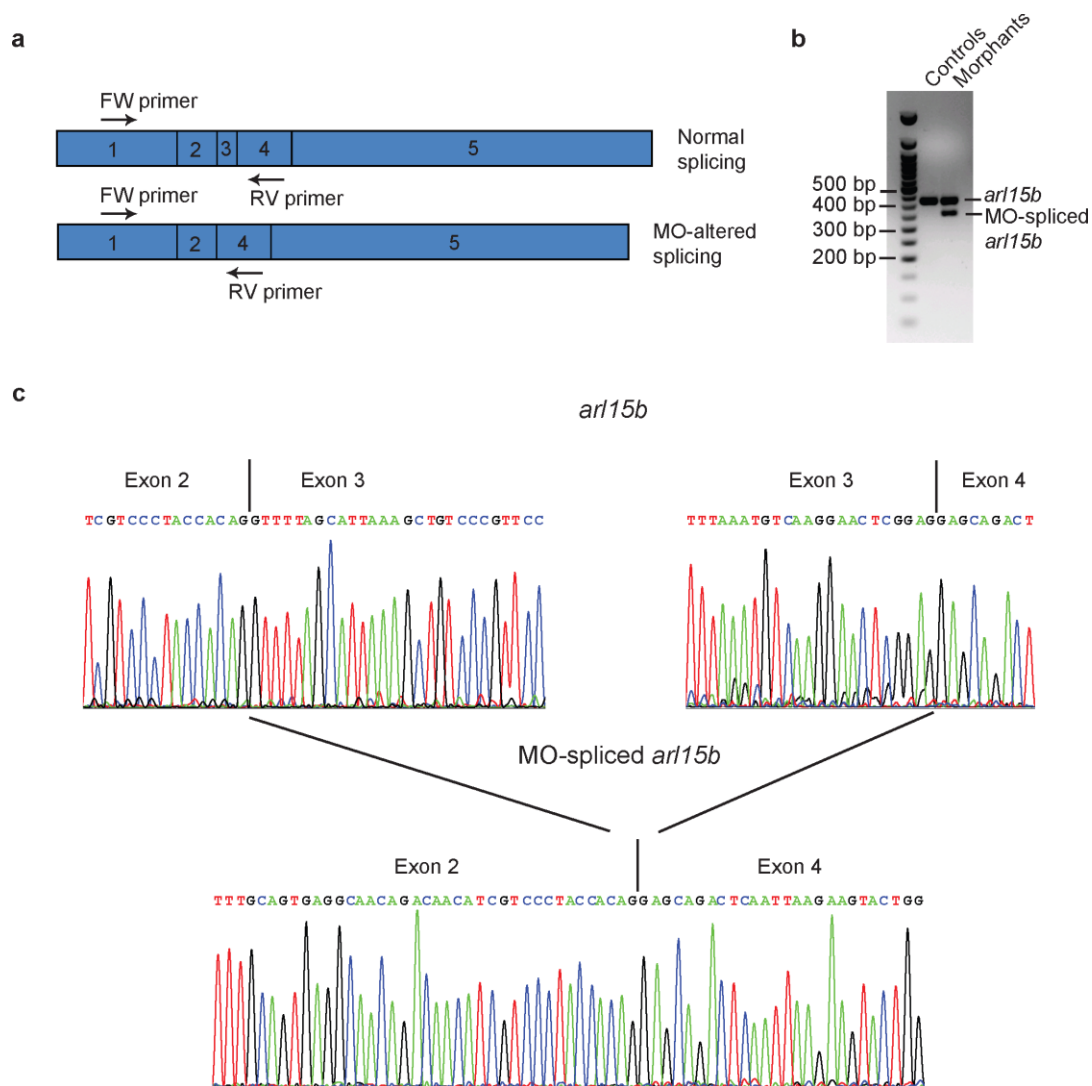
(**a**) Expected PCR products using forward (FW) and reverse (RV) primers located in exon 1 and 4 respectively on *arl15b* mRNA with normal splicing or altered splicing evoked by the *arl15b*-MO. (**b**) Gel electrophoresis image showing defects in the splicing process following injection of *arl15b*-MO (morphants, dose of 0.5 ng *arl15b*-MO/embryo) or control-MO (controls, dose of 0.5 ng control-MO/embryo). Bands showing correctly spliced *arl15b* mRNA and MO-spliced *arl15b* mRNA are shown. PCR was performed on cDNA prepared from larvae 5 days after injection. Shown on the left are the sizes (in bp) of the major bands of the DNA ladder. The expected amplicon size of the correctly spliced *arl15b* mRNA and the MO-spliced *arl15b* mRNA using FW and RV primers is of 411 bp and 351 bp respectively. (**c**)Chromatograms obtained from Sanger sequencing of the amplicons in the correctly spliced *arl15b* mRNA and the MO-spliced *arl15b* mRNA. The *arl15b*-MO evoked exon 3 skipping yielding a knockdown of Arl15b function. By skipping exon 3 with the *arl15b*-MO, the resulting protein lacks active domains such as the complete switch I region and part of the switch II region (switch regions are surface loops that undergo conformational changes upon GTP binding) and G3 box.

Supplementary Figure 10. Efficacy of the exon 4 skipping *arl15b*-MO used.
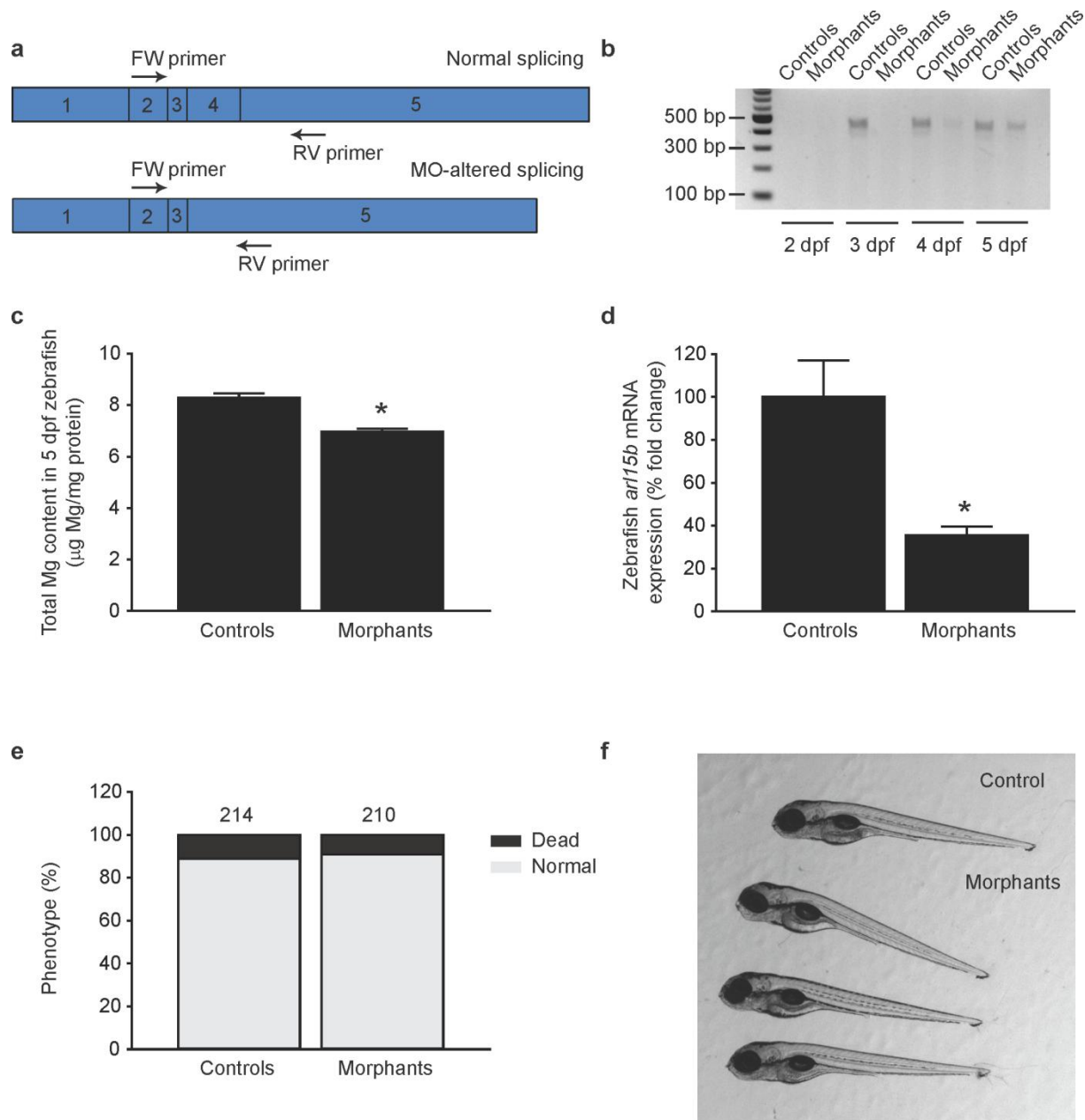
(**a**) Expected PCR products using forward (FW) and reverse (RV) primers located in exon 2 and 5 respectively on *arl15b* mRNA with normal splicing or altered splicing evoked by the *arl15b*-MO. (**b**) Gel electrophoresis image showing knockdown of *arl15b* gene expression following injection of *arl15b*-MO (morphants, dose of 2 ng *arl15b*-MO/embryo) or control-MO (controls, dose of 2ng control-MO/embryo) in 2-5 dpf zebrafish larvae. Bands showing correctly spliced *arl15b* mRNA are shown, while bands showing MO-spliced *arl15b* mRNA could not be detected so that the exon 4 skipping *arl15b*-MO evoked nonsense-mediated decay of *arl15b* transcripts. Shown on the left are the sizes (in bp) of the major bands of the DNA ladder. The expected amplicon size of the correctly spliced *arl15b* mRNA and the MO-spliced *arl15b* mRNA (not detected) using FW and RV primers is of 413 bp and 204bp respectively. (**c-f**) Characterization of the knockdown evoked by injection of 2 ng of exon 4 skipping *arl15b*-MO. Controls were injected with 2 ng of control-MO. **C,** total Mg content in

5 dpfmorphant and control zebrafish larvae. Data are presented as mean ± SEM (n = 10). *$P <$ 0.05 was considered statistically significant when compared with the control group. (**d**) Quantification of the knockdown evoked by the exon 4 skipping *arl15b*-MO by RT-qPCR using specific primers that discriminate for the correctly spliced (functional) *arl15b* mRNA. Data werecalculated using the Livakmethod ($2^{-\Delta\Delta Ct}$) and theyrepresent the mean folddifference (mean ± SEM,n= 10) from the control group (fish injected with the control-MO). *$P <$ 0.05 was considered statistically significant when compared with the control group. (**e**)Distribution of morphological phenotypes in the zebrafish larvae (5 dpf) used for the quantification of the *arl15b* knockdown by RT-qPCR. Numbers on top of the bars indicate the number of animals in each experimental condition. (**f**) Illustrative picture showing the characteristic phenotype (normal) evoked by knockdown of *arl15b* (2 ng/embryo of exon 4 skipping *arl15b*-MO).

SUPPLEMENTARY TABLES

Supplementary Table 1.Summary statistics for the genome-wide meta-analysis of serum Mg^{2+} levels.

	Effect allele	Other allele	Mean effect allele frequency	Effect size discovery (SE)	*P*value discovery	Effect size replica (SE)	*P*value replica	Effect size combined analysis (SE)	*P*value combined analysis	Direction of effects of individual cohorts	I^2
rs4460629	T	C	0.56	-0.144 (0.02)	4.89x10^{-13}	-0.100 (0.04)	1.15x10-2	-0.136 (0.018)	4.45x10^{-14}	--?-	14.6

The effect size sign for each individual cohort on the last but one column is represented by the sign – or +. The cohort displaying a "?" is for the Carlantino cohort, not having data for rs4460629. The last column shows the I^2 value, representing the heterogeneity across cohorts.

Supplementary Table 2. Urine (U) parameters in mice fed different Mg^{2+}-containing diets.

Baseline	Control diet (n=10)	Mg^{2+} deficient diet (n= 11)	Mg^{2+} excess diet (n=10)
Body weight (g)	23.7 ± 0.4	23.9 ± 0.8	25.6 ± 0.4*
Diuresis (µl/16h)	1307 ± 162	1467 ± 244	1985 ± 285
Diuresis (µl/min.gBW)	0.058 ± 0.007	0.066 ± 0.012	0.080 ± 0.012
U Na^+ (nmol/min)	164 ± 16	170 ± 19	177 ± 15
U K^+ (nmol/min)	413 ± 40	479 ± 42	501 ± 46
U Cl^- (nmol/min)	229 ± 21	263 ± 29	265 ± 26
U Mg^{2+} (nmol/min)	586 ± 59	621 ± 54	656 ± 78

Day 5	Control diet (n=10)	Mg^{2+} deficient diet (n= 11)	Mg^{2+} excess diet (n=10)
Body weight (g)	24.3 ± 0.5	24.3 ± 0.8	25.8 ± 0.5*
Diuresis (µl/16h)	1064 ± 49	1390 ± 168	$1126 \pm 132^{\neq}$
Diuresis (µl/min.gBW)	0.046 ± 0.002	0.060 ± 0.01	$0.045 \pm 0.005^{\neq}$
U Na^+ (nmol/min)	156 ± 14	171 ± 20	123 ± 20
U K^+ (nmol/min)	382 ± 36	393 ± 45	$327 \pm 52^{\neq}$
U Cl^- (nmol/min)	210 ± 20	239 ± 28	$168 \pm 30^{\neq}$
U Mg^{2+} (nmol/min)	478 ± 42	$13 \pm 3^{*,\neq}$	$1269 \pm 184^{*,\neq}$

Day 10	Control diet (n=10)	Mg^{2+} deficient diet (n= 11)	Mg^{2+} excess diet (n=10)
Body weight (g)	24.1 ± 0.4	24.3 ± 0.9	25.9 ± 0.5*
Diuresis (µl/16h)	$1516 \pm 136^{\S}$	1447 ± 149	$1334 \pm 124^{\neq}$
Diuresis (µl/min.gBW)	$0.066 \pm 0.006^{\S}$	0.062 ± 0.005	$0.053 \pm 0.005^{\neq}$
U Na^+ (nmol/min)	$189 \pm 16^{\S}$	176 ± 23	140 ± 18
U K^+ (nmol/min)	$532 \pm 46^{\S}$	465 ± 43	409 ± 51
U Cl^- (nmol/min)	$287 \pm 26^{\neq,\S}$	263 ± 33	$195 \pm 28^{*,\neq}$
U Mg^{2+} (nmol/min)	$723 \pm 49^{\S}$	$8.1 \pm 1.7^{*,\neq,\S}$	$1399 \pm 149^{*,\neq}$

*$P< 0.05$ versus control diet; $^{\neq}P < 0.05$ versus baseline; $^{\S}P< 0.05$ versus day 5

Supplementary Table 3. Plasma (P) parameters in mice fed different Mg^{2+}-containing diets.

Day 10	Control diet (n=10)	Mg^{2+} deficient diet (n= 11)	Mg^{2+} excess diet (n=10)
Body weight (g)	23.4 ± 0.5	23.3 ± 0.8	24.5 ± 0.6
P urea (mg/dl)	51.4 ± 1	$64.7 \pm 3.9*$	$52.0 \pm 2.6^{\neq}$
P creatinine (mg/dl)	0.07 ± 0.01	0.07 ± 0.01	0.08 ± 0.01
P Na^+ (mmol/l)	154 ± 1	$157 \pm 1*$	$152 \pm 1^{*,\neq}$
P K^+ (mmol/l)	4.0 ± 0.2	$4.4 \pm 0.1*$	$4.7 \pm 0.2*$
P Cl^- (mmol/l)	110 ± 1	111 ± 1	108 ± 1
P Ca^{2+} (mmol/l)	2.26 ± 0.03	$2.06 \pm 0.03*$	$2.29 \pm 0.03^{\neq}$
P Mg^{2+} (mg/dl)	2.95 ± 0.10	$1.08 \pm 0.11*$	$3.13 \pm 0.13^{\neq}$

$*P< 0.05$ versus control diet; $^{\neq} P < 0.05$ versus Mg^{2+}deficientdiet

Supplementary Table 4. Association of *ARL15* variants with metabolic phenotypes.

Source	Trait	SNP	p-value of association in published GWAS	Chr	Position	Gene Region	Context	PubMed	reference allele	p-value for uMg/uCreat in Meta-analysis	Beta for uMg/uCreat in Meta-analysis	Standard error of Beta for uMg/uCreat in Meta-analysis
dbGaP	Body Weight	rs2042313	2.45×10^{-7}	5	53212417	ARL15	Intron	17903300	NA	NA	NA	NA
dbGaP	Body Weight	rs2042313	5.15×10^{-7}	5	53212417	ARL15	Intron	17903300	NA	NA	NA	NA
NHGRI GWAS Catalog	Adiponectin	rs6450176	6.00×10^{-8}	5	53298025	ARL15	Intron	22479202	a	0.59	0.0091	0.0169
NHGRI GWAS Catalog	Cholesterol, HDL	rs6450176	5.00×10^{-8}	5	53298025	ARL15	Intron	20686565	a	0.59	0.0091	0.0169
NHGRI GWAS Catalog	Adiponectin	rs4311394	3.00×10^{-8}	5	53300662	ARL15	Intron	20011104	a	0.63	-0.0079	0.0165
dbGaP	Uric Acid	rs10513040	3.55×10^{-6}	5	53502295	ARL15	Intron	17903292	a	0.052	-0.0663	0.0341

Summary of previously associated SNPs in *ARL15* in published GWAS. The SNP associated with body weight is not present in our study. The 3 other SNPs are not significantly associated in the present uMg-to-creatinine meta-analysis, as shown in the last 3 columns.

Data were exported from dbGAP browser:http://www.ncbi.nlm.nih.gov/gap.

Supplementary Table 5. Study characteristics.

Study	CoLaus	INGI-Val Borbera	INGI-Carlantino	CROATIA-Vis	CROATIA-Korcula	CROATIA-Split	LBC1936
Sample size	5265	1541	281	195	889	489	660
Female % (N)	53%	56%	56.80%	58%	63.80%	56.50%	47.90%
Age, years mean (SD)	53.4 (10.7)	55 (18)	48 (19.7)	56.36 (15.5)	56.3 (13.9)	49.25 (14.7)	72.74 (0.75)
Serum Mg (mg/dl) mean (SD)	2.06 (0.166)	2.2 (0.3)	2.1 (0.2)	NA	2.04 (0.21)	NA	NA
Serum creatinine (mg/dl) mean (SD)	1.05 (0.24)	0.87 (0.25)	0.8 (0.2)	0.99 (0.32)	0.92 (0.18)	0.93 (0.15)	NA
Urine Mg (mg/dl) mean (SD)	6.9 (4.0)	8.4 (4.8)	8.1 (5)	5.93 (4.52)	7.6 (4)	8.76 (4.9)	8.70 (5.61)
Urine creatinine (mg/dl) mean (SD)	161.9 (81.4)	105.4 (59.1)	80.5 (42.1)	103.18 (65.8)	133.8 (63.8)	154.72 (72.98)	115.75 (62.20)
Urine Mg/creat ratio (mg/gr) mean (SD)	46.51 (25.98)	88.6 (36.5)	104.6 (44.8)	62.55 (33.37)	63.7 (32.5)	60.6 (26.8)	82.03 (42.23)
FEMg mean (SD)	3.27 (1.65)	5.2 (2.5)	6.0 (2.6)	NA	2.55 (1.33)	NA	NA
eGFR (mean, SD)	89.39 (20.03)	89.23 (23.28)	NA	89.41 (21.18)	87.72 (21.16)	94.92 (23.34)	NA

Supplementary Table 6. Study genotyping characteristics.

Study	CoLaus	INGI-Val Borbera	INGI-Carlantino	CROATIA-Vis	CROATIA-Korcula	CROATIA-Split	LBC1936
Array type	Affymetrix 500K	Illumina 370k	Illumina 370k	Illumina HumanHap300v1	Illumina HumanHap370CNV	Illumina HumanHap370CNV	Illumina 610
Genotype calling	BRLMM	BeadStudio analysis software	BeadStudio analysis software	Genome Studio	Genome Studio	Genome Studio	Genome studio
QC filters for genotyped SNPs used for imputation	pHWE<1e-7; individual call rate <90%; SNP call rate<70%; MAF<0.01	call rate >= 90%; MAF >= 1%; pHWE p > 0.0001	call rate >= 90%; MAF >= 1%; pHWE p > 0.0001	SNP Call rate<=0.98, MAF<0..01, pHWE<1e-6, Individual Call rate<0.95	SNP Call rate<=0.98, MAF<0..01, pHWE<1e-6, Individual Call rate<0.95	SNP Call rate<=0.98, MAF<0..01, pHWE<1e-6, Individual Call rate<0.95	pHWE<p < 1x10-3 individual call rate <95%; SNP call rate<98%; MAF<0.01
No of SNPs used for imputation	390'631	332'887	309'430	289'827	307'625	321'456	~500,000
Imputation	IMPUTE v0.2	MACH	MACH	MACH 1.0.16	MACH 1.0.16	MACH 1.0.16	MACH
Imputation Backbone for phased CEU haplotypes (NCBI build)	HapMap release 21 (build 35)	HapMap release 22 (build 36)	HapMap release 22 (build 36)	HapMap release 22 (build 36)	HapMap release 22 (build 36)	HapMap release 22 (build 36)	HapMap II (build 36)
Filtering of imputed genotypes	None	Rsq>0.3	Rsq>0.3	None	None	None	none
Data management	QUICKTEST	R, GenABEL, ProbABEL (mmscore	R, GenABEL, ProbABEL	R, GenABEL, ProbABEL	R, GenABEL, ProbABEL	R, GenABEL, ProbABEL	mach2qtl

and statistical analysis		function was used to account for relatedness)	(mmscorefunction was used to account for relatedness)	(mmscorefunction was used to account for relatedness)	(mmscore function was used to account for relatedness)	(mmscore function was used to account for relatedness)	
Population stratification or Principal Components	We included the first 3 principal components as covariates	We included the first 3 principal components as covariates	We included the first 3 principal components as covariates	We included the first 3 principal components as covariates	We included the first 3 principal components as covariates	We included the first 3 principal components as covariates	We included the first 4 principal components as covariates

Supplementary Table 7.Imputation status and quality for rs35929 and rs3824347.

SNP	COLAUS	CARLANTINO	KORCULA	LBC1936	SPLIT	VAL BORBERA	VIS
rs35929	I(0.95)	I (0.81)	I (1)	I(1)	I(1)	I(1)	I(1)
rs3824347	I(0.97)	I(0.76)	I(0.95)	I(0.97)	I(0.98)	I(0.97)	I(0.98)

Imputation status (G= genotyped, I=imputed) for both SNPs of interest in each cohort. Between brackets is the r^2 value representing imputation quality.

Supplementary Table 8.Primer oligonucleotide sequences used in the present study during RT-qPCR measurements.

Primer sequence 5' → 3'		Species	Amplicon size (bp)	Efficiency (%)
Actb		Mouse	102	102
Forward	TGCCCATCTATGAGGGCTAC			
Reverse	CCCGTTCAGTCAGGATCTTC			
Arl15		Mouse	133	98
Forward	TCATCAAGACAAGCCAGCAG			
Reverse	GCTGTCCTTCAGTGTGTCCA			
Gapdh		Mouse	176	104
Forward	TGCACCACCAACTGCTTAGC			
Reverse	GGATGCAGGGATGGGGGAGA			
Podocin		Mouse	162	103
Forward	GTCTAGCCCATGTGTCCAAA			
Reverse	CCACTTTGATGCCCCAAATA			
Pvalb		Mouse	136	97
Forward	GACGCCATTCTTCTGGAAAT			
Reverse	ATACCCCCACTGCCCTAAAA			
Arbp		Mouse	150	99
Forward	CTTCATTGTGGGAGCAGACA			
Reverse	TTCTCCAGAGCTGGGTTGTT			
Ncc		Mouse	148	101
Forward	CATGGTCTCCTTTGCCAACT			

Reverse	TGCCAAAGAAGCTACCATCA			
Nkcc2		Mouse	154	99
Forward	CCGTGGCCTACATAGGTGTT			
Reverse	GGCTCGTGTTGACATCTTGA			
Aqp2		Mouse	147	103
Forward	TCACTGGGTCTTCTGGATCG			
Reverse	CGTTCCTCCCAGTCAGTGT			
Ppia		Mouse	139	102
Forward	CGTCTCCTTCGAGCTGTTTG			
Reverse	CCACCCTGGCACATGAATC			
Hprt1		Mouse	162	99
Forward	ACATTGTGGCCCTCTGTGTG			
Reverse	TTATGTCCCCCGTTGACTGA			
Sglt2		Mouse	164	101
Forward	TTGGGCATCACCATGATTTA			
Reverse	GCTCCCAGGTATTTGTCGAA			
Trpm6		Mouse	156	100
Forward	CACAAGCCAGTGACCACCTA			
Reverse	GAGGCTCTTGAGGGCTTTTT			
Snat3		Mouse	109	99
Forward	GTTATCTTCGCCCCCAACAT			
Reverse	TGGGCATGATTCGGAAGTAG			
Alpha Enac		Mouse	151	96
Forward	CCTGGGCAGCTTCATCTTTA			

Reverse	GACTCCAGGCATGGAAGACA			
Casr		Mouse	150	97
Foward	CTCTGCTGCTTCTCCAGCT			
Reverse	GGCCTCAAATACCAGGAGGA			
Cabd28		Mouse	154	101
Forward	CTGACAGAGATGGCCAGGTT			
Reverse	AGCAAAGCATCCAGCTCATT			
arl15b		Zebrafish	133	104
Forward	AAGGAACTCGGAGGAGCAGACTCA			
Reverse	AGTGGAGCTCTGTACGCGCC			
elf1α		Zebrafish	89	100
Forward	GAGGCCAGCTCAAACATGGGC			
Reverse	AGGGCATCAAGAAGAGTAGTACCGC			

SUPPLEMENTARY REFERENCES

1. Firmann M, Mayor V, Vidal PM, Bochud M, Pécoud A, Hayoz D, Paccaud F, Preisig M, Song KS, Yuan X, Danoff TM, Stirnadel HA, Waterworth D, Mooser V, Waeber G, Vollenweider P: The CoLaus study: a population-based study to investigate the epidemiology and genetic determinants of cardiovascular risk factors and metabolic syndrome. *BMC Cardiovasc Disord* 8**:** 6, 2008.

2. Vitart V, Rudan I, Hayward C, Gray NK, Floyd J, Palmer CN, Knott SA, Kolcic I, Polasek O, Graessler J, Wilson JF, Marinaki A, Riches PL, Shu X, Janicijevic B, Smolej-Narancic N, Gorgoni B, Morgan J, Campbell S, Biloglav Z, Barac-Lauc L, Pericic M, Klaric IM, Zgaga L, Skaric-Juric T, Wild SH, Richardson WA, Hohenstein P, Kimber CH, Tenesa A, DonnellyLA, Fairbanks LD, Aringer M, McKeigue PM, Ralston SH, Morris AD, Rudan P, Hastie ND, Campbell H, Wright AF: SLC2A9 is a newly identified urate transporter influencing serum urate concentration, urate excretion and gout. *Nat Genet* 40**:** 437-442, 2008.

3. Polasek O, Marusić A, Rotim K, Hayward C, Vitart V, Huffman J, Campbell S, Janković S, Boban M, Biloglav Z, Kolcić I, Krzelj V, Terzić J, Matec L, Tometić G, Nonković D, Nincević J, Pehlić M, Zedelj J, Velagić V, Juricić D, Kirac I, Belak Kovacević S, Wright AF, Campbell H, Rudan I: Genome-wide association study of anthropometric traits in Korčula Island, Croatia. *Croat Med J* 50**:** 7-16, 2009.

4. Rudan I, Marusić A, Janković S, Rotim K, Boban M, Lauc G, Grković I, Dogas Z, Zemunik T, Vatavuk Z, Bencić G, Rudan D, Mulić R, Krzelj V, Terzić J, Stojanović D, Puntarić D, Bilić E, Ropac D, Vorko-Jović A, Znaor A, Stevanović R, Biloglav Z, Polasek O: "10001 Dalmatians:" Croatia launches its national biobank. *Croat Med J* 50**:** 4-6, 2009.

5. Deary IJ, Gow AJ, Taylor MD, Corley J, Brett C, Wilson V, Campbell H, Whalley LJ, Visscher PM, Porteous DJ, Starr JM: The Lothian Birth Cohort 1936: a study to examine influences on cognitive ageing from age 11 to age 70 and beyond. *BMC Geriatr* 7**:** 28, 2007.

6. Deary IJ, Gow AJ, Pattie A, Starr JM: Cohort profile: the Lothian Birth Cohorts of 1921 and 1936. *Int J Epidemiol* 41**:** 1576-1584, 2012.

7. Traglia M, Sala C, Masciullo C, Cverhova V, Lori F, Pistis G, Bione S, Gasparini P, Ulivi S, Ciullo M, Nutile T, Bosi E, Sirtori M, Mignogna G, Rubinacci A, Buetti I, Camaschella C, Petretto E, Toniolo D: Heritability and demographic analyses in the

large isolated population of Val Borbera suggest advantages in mapping complex traits genes. *PLoS One* 4**:** e7554, 2009.

8. Glaudemans B, Terryn S, Gölz N, Brunati M, Cattaneo A, Bachi A, Al-Qusairi L, Ziegler U, Staub O, Rampoldi L, Devuyst O: A primary culture system of mouse thick ascending limb cells with preserved function and uromodulin processing. *Pflügers Arch* 466**:** 343-356, 2014.

9. Hoenderop, JGJ, Dardenne, O, van Abel, M, van der Kemp, AW, van Os, CH, St -Arnaud, R, Bindels, RJM: Modulation of renal Ca^{2+} transport protein genes by dietary Ca^{2+} and 1,25-dihydroxyvitamin D_3 in 25-hydroxyvitamin D_3-1a-hydroxylase knockout mice. *FASEB J* 16**:** 1398-1406, 2002.

10. Ferrè, S, de Baaij, JHF, Ferreira, P, Germann, R, de Klerk, JB, Lavrijsen, M, van Zeeland, F, Venselaar, H, Kluijtmans, LA, Hoenderop, JGJ, Bindels, RJM: Mutations in PCBD1 cause hypomagnesemia and renal magnesium wasting. *J Am Soc Nephrol* 25**:** 574-586, 2014.

11. Nijenhuis, T, Hoenderop, JGJ, Loffing, J, van der Kemp, AWCM, van Os, CH, Bindels, RJM: Thiazide-induced hypocalciuria is accompanied by a decreased expression of Ca^{2+} transport proteins in kidney. *Kidney Int* 64**:** 555-564, 2003.

12. Voets T, Nilius B, Hoefs S, van der Kemp AW, Droogmans G, Bindels RJM, Hoenderop JGJ: TRPM6 forms the Mg^{2+} influx channel involved in intestinal and renal Mg^{2+} absorption. *J Biol Chem* 279**:** 19-25, 2004.

13. Groenestege WM, Hoenderop JGJ, van den Heuvel L, Knoers N, Bindels RJM: The epithelial Mg^{2+} channel transient receptor potential melastatin 6 is regulated by dietary Mg^{2+} content and estrogens. *J Am Soc Nephrol* 17**:** 1035-1043, 2006.

14. Wingert RA, Selleck R, Yu J, Song HD, Chen Z, Song A, Zhou Y, Thisse B, Thisse C, McMahon AP, Davidson AJ: The cdx genes and retinoic acid control the positioning and segmentation of the zebrafish pronephros. *PLoS Genet* 3**:** e189, 2007.

15. Wang Y-F, Tseng Y-C, Yan J-J, Hiroi J, Hwang P-P: Role of SLC12A10.2, a Na-Cl cotransporter-like protein, in a Cl uptake mechanism in zebrafish (*Danio rerio*). *Am J Physiol Regul Integr Comp Phys* 296**:** R1650-R1660, 2009.

16. Arjona FJ, Chen Y-X, Flik G, Bindels RJM, Hoenderop JGJ: Tissue-specific expression and in vivo regulation of zebrafish orthologues of mammalian genes related to symptomatic hypomagnesemia. *Pflügers Arch* 465**:** 1409-1421, 2013.

17. Hyatt TM, Ekker SC: Vectors and techniques for ectopic gene expression in zebrafish. In: *Methods in Cell biology,* edited by Detrich HW, Westerfield M, Zon LI, 1998, pp 117-126.

18. Mahmood F, Mozere M, Zdebik AA, Stanescu HC, Tobin J, Beales PL, Kleta R, Bockenhauer D, Russell C: Generation and validation of a zebrafish model of EAST (epilepsy, ataxia, sensorineural deafness and tubulopathy) syndrome. *Dis Model Mech* 6**:** 652-660, 2013.

19. Arjona FJ, de Baaij JHF, Schlingmann KP, Lameris ALL, van Wijk E, Flik G, Regele S, Korenke GC, Neophytou B, Rust S, Reintjes N, Konrad M, Bindels RJM, Hoenderop JGJ: CNNM2 mutations cause impaired brain development and seizures in patients with hypomagnesemia. *PLoS Genet* 10**:** e1004267, 2014.

20. Bustin SA, Benes V, Garson JA, Hellemans J, Huggett J, Kubista M, Mueller R, Nolan T, Pfaffl MW, Shipley GL, Vandesompele J, Wittwer CT: The MIQE guidelines. *Clin Chem* 55**:** 611-622, 2009.

21. Jouret F, Auzanneau C, Debaix H, Wada GH, Pretto C, Marbaix E, Karet FE, Courtoy PJ, Devuyst O: Ubiquitous and kidney-specific subunits of vacuolar H+-ATPase are differentially expressed during nephrogenesis. *J Am Soc Nephrol* 16**:** 3235-3246, 2005.

22. Parreira KS, Debaix H, Cnops Y, Geffers L, Devuyst O: Expression patterns of the aquaporin gene family during renal development: influence of genetic variability. *Pflügers Arch* 458**:** 745-759, 2009.

23. McCurley AT, Callard GV: Characterization of housekeeping genes in zebrafish: male-female differences and effects of tissue type, developmental stage and chemical treatment. *BMC Mol Biol* 9**:** 102, 2008.